Journal of the European Ceramic Society **19** (1999) 797–801

PII: S0955-2219(98)00317-3
0955-2219/99/$ - see front matter

Measurement of Conductivity Profiles in Acceptor-doped Strontium Titanate

S. Rodewald, J. Fleig* and J. Maier

Max-Planck-Institut für Festkörperforschung, Stuttgart, Germany

Abstract

Spatially resolved microcontact impedance spectroscopy using circular microelectrodes is applied to acceptor-doped $SrTiO_3$. It is demonstrated that local bulk conductivities can be obtained with a spatial resolution down to the 10 μm range. In particular, conductivity profiles in electrocolored samples are measured, revealing a very characteristic profile shape. An existing model for the resistance degradation in $SrTiO_3$ could be confirmed by this experiment. Measurements in polycrystalline material yield conductivity variations within single grains which can be related to oxygen vacancy blocking at grain boundaries and the corresponding stoichiometry variations.

Keywords: microelectrodes, grain boundaries, electrical conductivity, impedance, titanates.

1 Introduction

Electroceramic materials frequently exhibit spatially varying electrical conductivities caused by inhomogeneous impurity concentrations, gradients in the native stoichiometry, etc. Conductivity profiles as a consequence of stoichiometry variations are well-known in mixed conductors and arise, e.g. if samples are quenched before reaching equilibrium with the surrounding gas phase, by kinetic effects during cooling or as a consequence of electrical polarization with electrodes which block one charge carrier.[1] This Wagner–Hebb–Polarization can play an important role in resistance degradation of perovskite-type titanates (electrocoloration).[2,3]

Spatially resolved measurements to detect such conductivity profiles using microelectrodes are quite common in covalent semiconductors such as Si[4] and GaAs[5] but very rare in highly resistive mixed or ionic conductors. This is connected with the fact that rather high resistances are involved and that, moreover, an impedance spectroscopy analysis is necessary to separate electrode and bulk contributions from the overall resistance to obtain reliable information. On the other hand, microcontact impedance spectroscopy can be a very useful tool to detect inhomogeneities in mixed or ionic conductors as shown for AgCl by measuring a diffusion profile of the $CdCl_2$ dopant[6] or by detecting enhanced conductivity along grain boundaries.[7] In this contribution we demonstrate that the technique can be used to perform spatially resolved conductivity measurements on acceptor-doped $SrTiO_3$. Beside the aim to prove the applicability of the method emphasis is put on the analysis of conductivity profiles caused by high electric fields (electrocoloration).

2 Experimental

Fe-doped $SrTiO_3$ single crystals (0·22 mol% Fe) and polycrystals (0·2 mol% Fe) were used in these investigations. The single crystals grown by the Verneuil technique, were purchased from Frank & Schulte GmbH (Essen, FRG) and the polycrystalline material was prepared by the mixed oxide technique with $SrCO_3$, TiO_2 and $Fe(NO_3)_3 \cdot 9H_2O$ as starting material. The crystal boule and the polycrystalline pellets were cut into slices of 5–8 mm length and a thickness of about 1 mm. All samples were equilibrated in air at 1273 K for 8 h. Circular microelectrodes on top of the sample (mostly 10 to 20 μm diameter) were prepared by a lithographic lift-off process from an evaporated 20 nm Cr/200 nm Au film. A picture of microelectrodes on a $SrTiO_3$ polycrystal is shown in Fig. 1. As a counterelectrode on the backside a dense 20 nm Cr/200 nm Au film was evaporated. Two further Cr/Au electrode stripes on the sides of the

*To whom correspondence should be addressed. Fax: +49-711-689-1722; e-mail: fleig@chemix.mpi-stuttgart.mpg.de

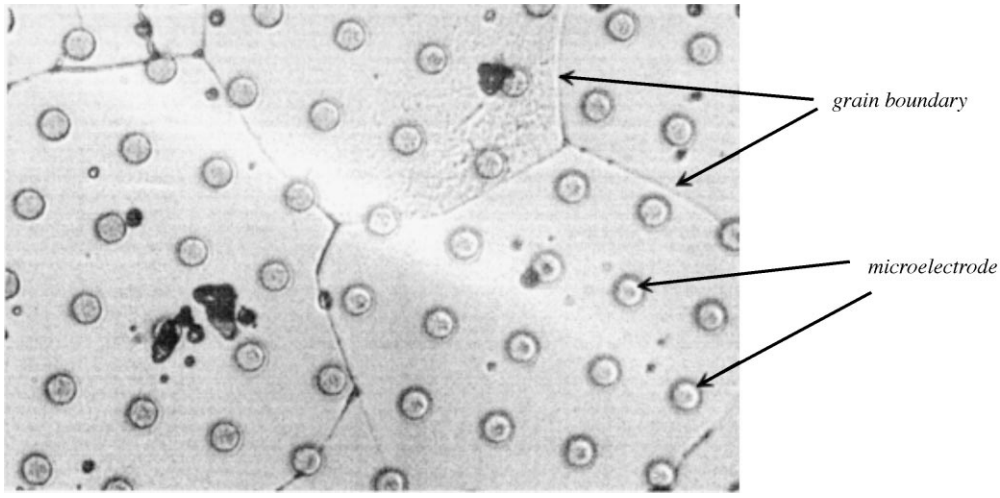

Fig. 1. Cr/Au-microelectrodes with a diameter of 10 μm evaporated on an iron-doped $SrTiO_3$ polycrystalline sample. The dark imprints of some electrodes are due to contacting with tungsten tips.

samples were used to perform the electrocoloration procedure: These two stripe were connected to a Keithley 237 high voltage unit and an electrical field of 100 V cm^{-1} was applied for 30 to 120 min at a temperature of 493–500 K. This leads to a significant movement of a dark colorfront in the sample. The electrocoloration electrodes were disconnected and the established profile was determined at different temperatures (413–473 K) by subsequently contacting microelectrodes in a line with a tungsten tip and measuring the impedance spectrum between microelectrode and the counter-electrode on the backside. Due to the high impedances of up to 1000 GΩ a home-made impedance converter has to be used in combination with a Solartron 1260 FRA.

3 Applicability of the method

Several problems can emerge when applying spatially resolved microcontact impedance spectroscopy to a new material as e.g. poor adhesion of the microelectrodes (for Pt). The possibly most serious problem deals with the fact that the measured bulk resistance can be strongly distorted by 'leakage' currents along highly conducting surface layers. Such effects are much more pronounced in this case than in macroscopic measurements and can even be used to sensitively measure the conductivity of highly conducting surface layers.[8] To exclude the influence of such layers it is necessary to compare the conductivities obtained by microelectrodes and by 'macroelectrodes'.

In the absence of additional surface effects the resistance R_{mic} between a microelectrode with diameter d and an extended counter electrode is given by[9]

$$R_{\mathrm{mic}} = \frac{1}{2d\sigma_{\mathrm{bulk}}} \tag{1}$$

with σ_{bulk} being the bulk conductivity. Figure 2 shows the temperature dependent bulk conductivity calculated from a microcontact measurement according to eqn (1) and the conductivity of the same sample as obtained from a measurement using macroscopic electrodes. In the entire temperature range the agreement between the two values is satisfactory.

Both the microscopic and the macroscopic bulk resistances are gained from the high-frequency semicircles of the impedance spectra (Fig. 3). The main difference between microscopic and macroscopic spectra are (i) the absolute value of the resistances and (ii) the much more pronounced electrode impedance for microelectrodes. The strong increase of electrode contributions for smaller electrodes is due to the fact that the electrode resistance is inversely proportional to d^2 while the bulk resistance is inversely proportional to d. The latter proportionality can also be seen in Fig. 4(a): Within the accuracy of the measurement (resistance variation for different contacts of identical shape $\approx \pm$ 15%) the proportionality is confirmed. Hence the finite thickness of the sample plays no role (as long as the thickness is much larger than the contact diameter). In principle the bulk capacitance C_{mic} reads

$$C_{\mathrm{mic}} = 2\varepsilon_{\mathrm{bulk}} d \tag{2}$$

with $\varepsilon_{\mathrm{bulk}}$ being the bulk permittivity and the proportionality of d and capacitance could also be confirmed with an offset for $d \rightarrow 0$ due to stray capacitances of 100–300 fF [cf. Fig. 4(b)]. However, it has to be emphasized that most materials have

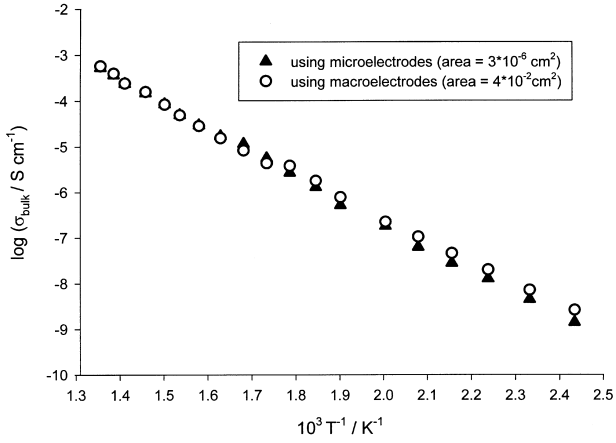

Fig. 2. The applicability of microcontact impedance spectroscopy is evidenced by the agreement of the bulk conductivity σ_{bulk} obtained from the resistances (R) by impedance measurements with macroscopic electrodes ($\sigma_{bulk} = \lambda D/R \times A : A$, electrode area D, sample thickness; λ, correction factor determined by finite element calculation) and microelectrodes ($\sigma_{bulk} = 1/2 \times R \times d$; d, electrode diameter = 20 μm).

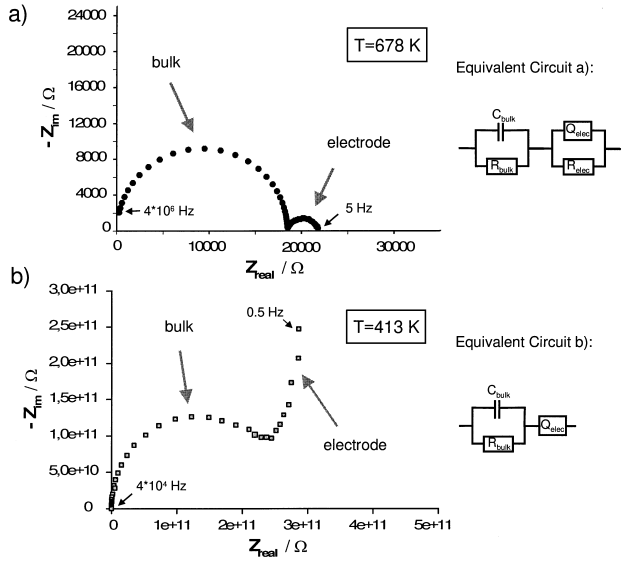

Fig. 3. Impedance spectra of a sample measured with (a) macroscopic electrodes (5–4×10^6 Hz) and (b) microelectrodes (0·5–4×10^4 Hz). The equivalent circuits used for analysing the impedance data are sketched beside the spectra. Symbol Q represents a 'Constant Phase Element'.

smaller permittivities than $SrTiO_3$ and the capacitance of the first semicircle in the impedance plot is often dominated by residual stray capacitances.

Equations (1) and (2) are distinctly modified if surface layers play a role. Hence, these tests prove that enhanced surface conductivities do not distort the results and that microcontact impedance spectroscopy can be applied to $SrTiO_3$ in order to obtain spatially resolved conductivity data.

4 Measurement of conductivity profiles

An exact evaluation of the bulk conductivity according to eqn (1) requires a homogeneous sample and hence conductivity profiles are expected to lead to modifications. On the other hand, most of the bulk resistance drops in a very small region beneath the microcontact: For a hemispherical electrode (radial current lines) with 10 μm diameter 75% of the bulk resistance drops within a distance of 15 μm from the electrode. Hence, the evaluation of spatially resolved measurements according to eqn (1) is still possible with a spatial resolution of approximately two times the microcontact diameter. For very sharp profiles, however, conductivities calculated from eqn (1) reflect mean values.

In this contribution we use the microcontact impedance spectroscopy to investigate the well-known phenomena of electrocoloration in $SrTiO_3$ caused by high electric fields. Much work on this topic has been done by Waser *et al.*[2,10–12] who could show that the experimental observations can be understood by a model which assumes oxygen vacancies being blocked at the electrodes (Wagner–Hebb–Polarisation) and hence the build-up of a stoichiometry profile in $SrTiO_3$. However, a direct

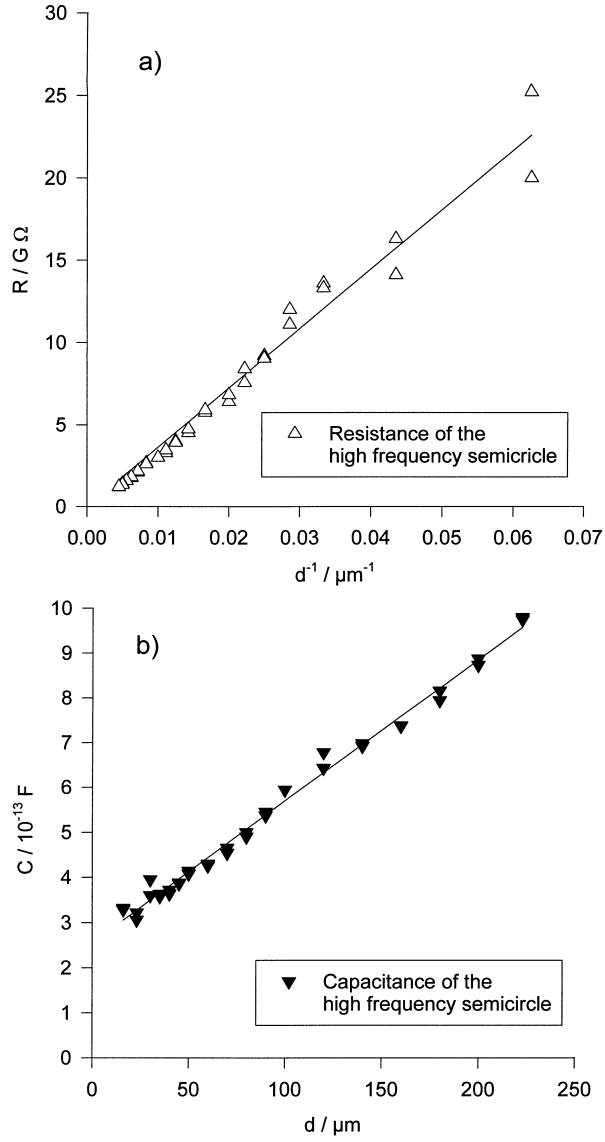

Fig. 4. (a) Resistance and (b) capacitance of the high-frequency semicircle versus microelectrode diameter for T = 473 K.

measurement of conductivity profiles connected with these stoichiometry variations had not been performed yet.

We measured the conductivity variations in electrocolored samples at different temperatures and observed pronounced profiles with a rather characteristic shape. A cathodic as well as an anodic increase of the conductivity appears with a plateau in between. Moreover, a conductivity 'dip' emerges (Fig. 5), the depth of which is temperature dependent. Using a finite difference algorithm according to Ref.1 and the material parameters of $SrTiO_3$[13] the entire shape including the 'dip' could be quantitatively simulated. The underlying model assumes blocking electrodes for oxygen vacancies and consequently an accumulation of oxygen vacancies at the cathode and a depletion of oxygen vacancies at the anode. This leads to an n-type conducting region at the cathode and an enhanced p-conduction at the anode. The conductivity plateau is due to ionic conductivity in a region with undisturbed (constant) oxygen vacancy concentration and the 'dip' reflects the vacancy depletion close to the electrocoloration anode with the hole conduction taking over the total conductivity in the minimum. Hence the model suggested by Baiatu *et al.*[2] to explain electrocoloration in acceptor-doped $SrTiO_3$ is confirmed. A more detailed discussion of the measured profiles and their temperature and time dependences will be given in a forthcoming paper.[14]

According to experimental observations[12,15] grain boundaries are supposed to strongly influence the electrocoloration process. Hence also modifications of the conductivity profiles could be expected in polycrystals. Such modifications could be observed in the conductivity profile: While in an electrocolored single crystal the profile was relatively smooth, considerable fluctuations of the conductivity values along a decreasing conductivity profile were measured in a polycrystal (Fig. 6). These variations cannot be explained by dopant inhomogeneities in the ceramics since a smooth conductivity distribution was observed before electrocoloration. However, a correlation between grain boundaries and conductivity peaks is obvious. Some grains show an enhanced conductivity close to the grain boundary, and particularly the large grain (r.h.s. in Fig. 6) exhibits a distinct profile which superimposes the overall profile. This can be explained by a hindrance for the oxygen vacancy transport across the grain boundary leading to a pile-up of vacancies on one side and a depletion of vacancies on the other side of the boundary and thus to an increased electronic conductivity on both sides of each grain boundary.[12] Moreover, there is some indication from the profile that not all grain boundaries have the same blocking effect for oxygen vacancies. These measurements are still in progress and a detailed discussion will be given in a forthcoming paper.[14]

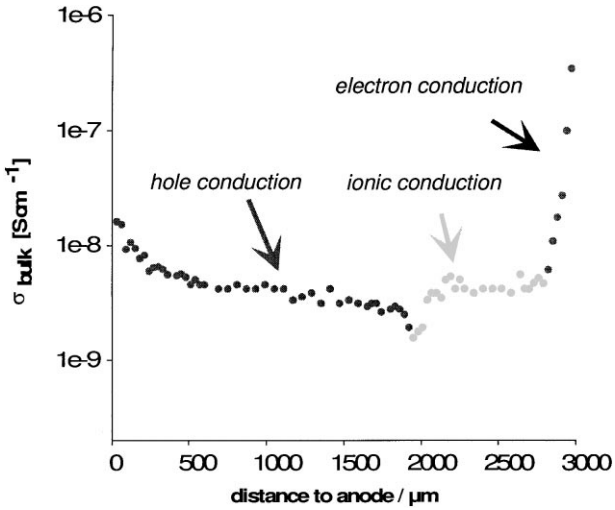

Fig. 5. Part of the bulk conductivity profile in an iron-doped $SrTiO_3$ single crystal after electrocoloration ($E = 100\,V\,cm^{-1}$) at 493 K for 90 min. The conductivity measurement was performed at 417 K after the electrocoloration.

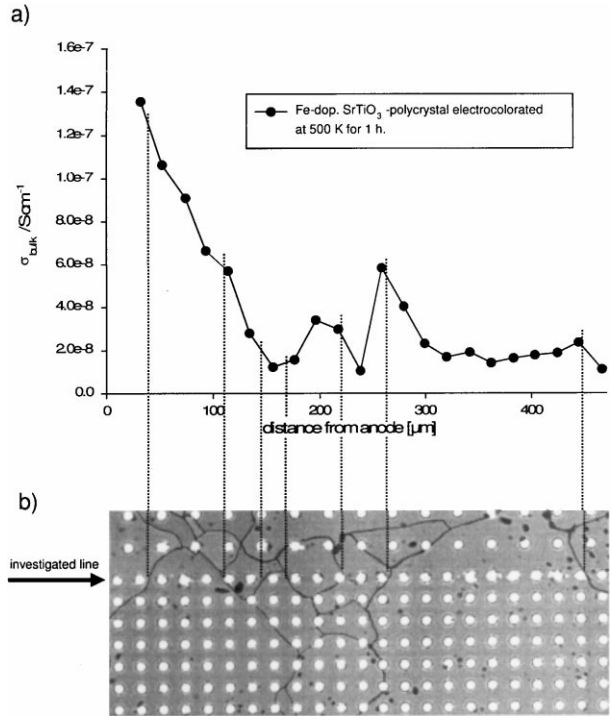

Fig. 6. Bulk conductivity profile in an electrocolorated Fe-doped $SrTiO_3$ polycrystal ($E = 100\,V\,cm^{-1}$, coloration at 500 K for 60 min). The corresponding area of the sample with evaporated microelectrodes ($d = 10\,\mu m$) is depicted below the diagram. The dotted lines indicate grain boundaries. The profile was measured at 470 K.

5 Conclusions

It could be shown that spatially resolved microcontact impedance spectroscopy can be applied to acceptor-doped $SrTiO_3$ in order to obtain local

conductivities and hence conductivity profiles with a resolution in the range of 10 μm. Spatially resolved conductivity measurements in electrocolored samples revealed very characteristic shapes and confirmed the electrochemical polarization model which assumes blocked oxygen vacancies at both electrodes causing a stoichiometry profile. Conductivity variations within single grains are found, which confirm the blocking character of grain boundaries in acceptor-doped $SrTiO_3$.

References

1. Yokota, I., *J. Phys. Soc. Japan* 1961, **16**, 2213–2223.
2. Baiatu, T., Waser, R. and Härdtl, K.-H., *J. Am. Ceram. Soc.*, 1990, **73**, 1663–1673.
3. Blanc, J. and Staebler, D. L., *Phys. Rev.*, 1971, **B4**, 3548–3557.
4. Mazur, R. G. and Dickey, D. H., *J. Electrochem. Soc.*, 1967, **114**, 255–259.
5. Frank, H. and Azim, S. A., *Solid State Electronics*, 1967, **10**, 727–728.
6. Fleig, J. and Maier, J., *Solid State Ionics*, 1996, **85**, 9–15.
7. Jamnik, J., Fleig, J. and Maier, J., *Mat. Res. Soc. Symp. Proc,* 1996, **411**, 25–30.
8. Fleig, J., Noll, F. and Maier, J., *Ber. Bunsenges. Phys. Chem.*, 1996, **100**, 607–615.
9. Holm, R., *Electric Contacts*. Springer–Verlag, Berlin, 1967, p. 16.
10. Raith, A., Reijinen, P. and Waser, R., *Ber. Bunsenges. Phys. Chem.,* 1988, **92**, 1516–1522.
11. Waser, R., Baiatu, T. and Härdtl, K.-H., *J. Am. Ceram. Soc.*, 1990, **73**, 1654–1662.
12. Waser, R., Baiatu, T. and Härdtl, K.-H., *J. Am. Ceram. Soc.*, 1990, **73**, 1645–1653.
13. Denk, I., Münch, W. and Maier, J., *J. Am. Ceram. Soc.*, 1995, **78**, 3265–3272.
14. Rodewald, S., Fleig, J. and Maier, J., in preparation.
15. Denk, I., Claus, J. and Maier, J., *J. Electrochem. Soc.,* 1997, **144**, 3526–3536.